Cerebral Cortex, February 2022;32: 329–341

https://doi.org/10.1093/cercor/bhab211
Advance Access Publication Date: 31 July 2021
Original Article

ORIGINAL ARTICLE

Thyroid Hormone Transporter Deficiency in Mice Impacts Multiple Stages of GABAergic Interneuron Development

Steffen Mayerl[1,2,3], Jiesi Chen[1,4], Eva Salveridou[3,4], Anita Boelen[5], Veerle M. Darras[6] and Heike Heuer[1,3,4]

[1]Leibniz Institute on Aging/Fritz Lipmann Institute, 07745 Jena, Germany, [2]MRC Centre for Regenerative Medicine, University of Edinburgh, Edinburgh EH16 4UU, UK, [3]Department of Endocrinology, Diabetes and Metabolism; University Duisburg-Essen, 45147 Essen, Germany, [4]Leibniz Research Institute for Environmental Medicine, 40225 Düsseldorf, Germany, [5]Endocrinology Laboratory, Department of Clinical Chemistry, Amsterdam Gastroenterology & Metabolism, Amsterdam UMC, University of Amsterdam, 1105 AZ Amsterdam, the Netherlands and [6]Laboratory of Comparative Endocrinology, Animal Physiology and Neurobiology Section, Biology Department, Katholieke Universiteit Leuven, 3000 Leuven, Belgium

Address correspondence to Steffen Mayerl University Hospital Essen, University Duisburg-Essen, Hufelandstraße 55, 45147 Essen, Germany. Email: steffen.mayerl@uk-essen.de

Abstract

Cortical interneuron neurogenesis is strictly regulated and depends on the presence of thyroid hormone (TH). In particular, inhibitory interneurons expressing the calcium binding protein Parvalbumin are highly sensitive toward developmental hypothyroidism. Reduced numbers of Parvalbumin-positive interneurons are observed in mice due to the combined absence of the TH transporters Mct8 and Oatp1c1. To unravel if cortical Parvalbumin-positive interneurons depend on cell-autonomous action of Mct8/Oatp1c1, we compared Mct8/Oatp1c1 double knockout (dko) mice to conditional knockouts with abolished TH transporter expression in progenitors of Parvalbumin-positive interneurons. These conditional knockouts exhibited a transient delay in the appearance of Parvalbumin-positive interneurons in the early postnatal somatosensory cortex while cell numbers remained permanently reduced in Mct8/Oatp1c1 dko mice. Using fluorescence in situ hybridization on E12.5 embryonic brains, we detected reduced expression of sonic hedgehog signaling components in Mct8/Oatp1c1 dko embryos only. Moreover, we revealed spatially distinct expression patterns of both TH transporters at brain barriers at E12.5 by immunofluorescence. At later developmental stages, we uncovered a sequential expression of first Oatp1c1 in individual interneurons and then Mct8 in Parvalbumin-positive subtypes. Together, our results point to multiple cell-autonomous and noncell-autonomous mechanisms that depend on proper TH transport during cortical interneuron development.

Key words: Allan Herndon Dudley Syndrome, GABAergic interneurons, Mct8, Oatp1c1, Slc16a2, Slco1c1, Parvalbumin, thyroid hormone

Introduction

GABAergic interneuron-mediated inhibition is pivotal for stable neuronal networks and a proper functioning of the cerebral cortex (Wonders and Anderson 2006; Rossignol 2011; Powell 2013). Hence, impairments in the generation of interneurons, their specification, migration, and synapse formation are associated with developmental disorders like autism spectrum disorder, schizophrenia, or childhood epilepsy (Levitt, Eagleson, and Powell 2004; Wonders and Anderson 2006). Thyroid hormone (TH) is a major external signaling cue that governs the formation of interneurons. Consequently, maternal hypothyroidism has been linked to disruptions in the generation of a specific subset of inhibitory interneurons expressing the Calcium binding protein Parvalbumin (PV) in the offspring that manifests in an increased seizure susceptibility later in life (Berbel et al. 1996; Gilbert et al. 2007; Wallis et al. 2008; Richard et al. 2020). Likewise, patients with mutations in the TH-transporting monocarboxylate transporter 8 (MCT8), also known as Allan-Herndon-Dudley Syndrome (AHDS), show a reduced number of PV positive interneurons and a predisposition toward seizures putatively due to an impaired TH transport into the CNS and/or neural target cells (Dumitrescu et al. 2004; Schwartz et al. 2005; Lopez-Espindola et al. 2014; Friesema et al. 2004). In fact, similar deficits in interneuron formation were recapitulated in the murine AHDS model of Mct8/Organic anion transporting polypeptide 1c1 (Oatp1c1) double deficiency (Mayerl et al. 2014). The reduced appearance of PV positive neurons is suggestive for a generally altered inhibition in cortical circuits that may represent one major pathogenic mechanism driving the neurological phenotype of AHDS (Remerand et al. 2019). The key question as to whether these perturbations result from a cell autonomous requirement of both TH transporters during interneuron development remains elusive. Addressing this, however, is instrumental in advancing our understanding of why AHDS patients are prone to epileptic seizures.

In mice, interneuron neurogenesis is a spatially and temporally tightly regulated process that takes place in the ventral telencephalon between embryonic days E12.5 and E16.5 (Wonders and Anderson 2006). Subsequently, newly formed interneurons first migrate tangentially through the neocortex, followed by radial migration to their predestined cortical layer before they mature and integrate functionally into the existing cortical network (Wonders and Anderson 2006; Rossignol 2011). Distinct regions within the ventral telencephalon give rise to specific subpopulations of GABAergic interneurons: Calretinin positive (CR+) bitufted interneurons are born in the caudal ganglionic eminence (CGE) whereas PV+ basket and chandelier cells as well as Somatostatin (SST) + Martinotti and non-Martinotti cells originate from the adjacent medial ganglionic eminence (MGE) (Xu et al. 2004; Butt et al. 2005; Wonders and Anderson 2006). The specification of these different subpopulations of interneurons that constitute the major subtypes in the cerebral cortex depends on the interplay of transcription factors and gradients of morphogens. A well-studied example is the strict dependence of MGE-derived PV+ and SST+ cells on the transcription factor Nkx2.1 whose absence virtually abolishes the generation of the aforementioned cell populations (Wonders and Anderson 2006). Nkx2.1 expression in turn is maintained by the morphogen sonic hedgehog (Shh) that regulates cortical interneuron identity (Xu, Wonders, and Anderson 2005; Xu et al. 2010).

Here, we have addressed if Mct8/Oatp1c1 deficiency interferes with the proper specification of interneuron subtypes either in a cell-autonomous manner due to the absence of TH transporters in progenitor cells or in a noncell-autonomous manner by altering specification cues in the local environment. To distinguish between these 2 possibilities, we generated mice with conditional deletion of Mct8/Oatp1c1 in Nkx2.1 positive progenitor cells and compared them to Mct8/Oatp1c1 dko mice. Loss of Mct8 and Oatp1c1 in Nkx2.1 expressing precursor cells as well as global deletion of both TH transporters culminated in a significantly reduced number of PV+ interneurons at P12 whereas CR+ interneurons were more numerous. Although these changes were sustained at later time points in Mct8/Oatp1c1 dko mice, cell numbers normalized in the conditional knockout mice pointing to noncell-autonomous effects of TH transporters in interneuron differentiation. Moreover, we unraveled specific effects on the Shh signaling pathway in the MGE of the global double knockout model only.

Materials and Methods

Animals

Mct8 fl/fl (or Mct8 fl/y) and Oatp1c1 fl/fl mice were generated and genotyped as described elsewhere (Mayerl et al. 2012; Mayerl et al. 2018) and mated with transgenic animals expressing a constitutively active Cre recombinase driven by the Nkx2.1 promoter (Xu, Tam, and Anderson 2008) as well as mice harboring a Cre reporter allele consisting of a loxP-flanked STOP cassette that prevents transcription of a CAG promotor driven EYFP construct (Gt(ROSA)26Sor$^{tm3(CAG-EYFP)Hze}$) (Madisen et al. 2010). Detection of the Nkx2.1-Cre and the EYFP transgene was performed as stated elsewhere (Xu, Tam, and Anderson 2008; Madisen et al. 2010). Mct8 fl/fl; Nkx2.1-Cre; EYFP (short: Mct8 fl Cre), Oatp1c1 fl/fl; Nkx2.1-Cre; EYFP (short Oatp1c1 fl Cre), and Mct8 fl/fl; Oatp1c1 fl/fl; Nkx2.1-Cre; EYFP (short: M/O dfl Cre) were analyzed. The Nkx2.1-Cre allele was transmitted through the paternal lineage only to circumvent TH transporter ablation in the thyroid gland of the dam that may lead to altered maternal serum TH levels and consequently impact fetal development. As controls, mice carrying both Nkx2.1-Cre and EYFP transgenes on a Mct8/Oatp1c1 wild-type (wt) background were used (Mct8 wt; Oatp1c1 wt; Nkx2.1-Cre; EYFP; short: control). Likewise, animals on a Mct8/Oatp1c1 double knockout background (Mayerl et al. 2014) were bred with Nkx2.1-Cre and EYFP positive animals to produce Mct8 ko/ko; Oatp1c1 ko/ko; Nkx2.1-Cre; EYFP mice (short: M/O dko; Cre). Animals for analysis were obtained from breeding Mct8 wt/ko; Oatp1c1 ko/ko; Nkx2.1-Cre negative; EYFP females with Mct8 ko/y; Oatp1c1 ko/ko; Nkx2.1-Cre tg; EYFP males. Using Gpower3.1, a priori power calculation was performed based on previous data (Mayerl et al. 2014; Desouza et al. 2011) to determine the minimum number of animals needed.

Mice were kept at constant temperature (22°C) on a 12 h light, 12 h dark cycle and were provided with standard laboratory chow and water ad libitum. For determination of serum and forebrain TH levels at P12, animals were deeply anesthetized with isoflurane. Blood samples were taken and animals were intracardially perfused with PBS. Serum TH was measured as stated elsewhere (Wiersinga and Chopra 1982; de Vries et al. 2016). Forebrain T4 and T3 content were assessed at P12 following rough homogenization and extraction of the tissues as described by Reyns et al. (2002) and detailed in the Supplementary information. For immunofluorescence studies, mice were deeply anesthetized with isoflurane and transcardially perfused with 4% PFA at indicated time points. At P28, only male mice

were analyzed; for earlier time points both sexes were used. Animals were harvested from at least 2 litters from 2 independent breeding pairs.

To generate E12.5 embryos, Mct8 fl/fl Oatp1c1 fl/fl (= M/O dfl) females were mated with M/O dfl Cre males followed by plug-reading. Pregnant females were sacrificed by cervical dislocation. Embryos were decapitated and heads were frozen in isopentane on dry ice. Genotyping of the offspring was conducted by PCR. The resulting Cre negative animals were used as controls for Cre positive littermates. Mct8 wt/ko; Oatp1c1 ko/ko females were bred with Mct8 ko/y; Oatp1c1 ko/ko males and the resulting M/O dko animals were utilized. In each case, tissue was collected from 3 litters. Wild-type breeding pairs have been used for the collection of E14.5 and E18.5 embryos. Offspring at P0 were generated as described above. Animals were decapitated, heads (E14.5, E18.5) or isolated brains (P0) were either freshly frozen or fixed for 72 h in 4% PFA, dehydrated in 30% sucrose and frozen in isopentane on dry ice. Animals were harvested from 2 litters per time point.

All animal studies were executed in accordance with the European Union (EU) directive 2010/63/EU and approved by the Animal Welfare Committee of the Thüringer Landesamt für Lebensmittelsicherheit und Verbraucherschutz (TLLV; Bad Langensalza, Germany), the Landesamt für Natur, Umwelt und Verbraucherschutz Nordrhein-Westfalen (LANUV; Recklinghausen, Germany) as well as in compliance with local guidelines by the University Hospital Essen.

Immunofluorescence Studies

Perfusion-fixed forebrains were cut into 50 µm frontal sections on a vibratome (MICROM GmbH, Walldorf, Germany). Sections (Bregma 1.0 to −0.55) were blocked and permeabilized with 10% normal goat serum in 0.2% Triton X-100 containing PBS. Consecutive forebrain sections were stained with the following antibodies: rabbit anti-Calretinin (Millipore; 1:500), mouse anti-glutamate decarboxylase 67 kD (GAD67; Millipore; 1:200), chicken anti-GFP (Aves Labs; 1:500), mouse anti-PV (Millipore; 1:1000), rabbit anti-Somatostatin (Immunostar; 1:100). Subsequently, sections were incubated with respective Alexa Fluor 488- or Alexa Fluor 555-labeled secondary antibodies raised in goat (Invitrogen; all 1:1000) and with Hoechst33258 (1:10 000, Invitrogen) to label cell nuclei. Images were taken using an Olympus AX70 microscope.

For visualization of TH transporters, fresh-frozen or PFA-fixed E12.5, E14.5, E18.5 heads as well as P0 brains were used. 20 µm thick cryosections were produced on a Cryostat (Leica). For Mct8 detection, sections were post-fixed for 10 min in 4% PFA, washed in PBS, incubated for 10 min in PBS containing 0.1% Triton X-100 and 0.1 M Glycin and blocked with 10% normal goat serum in 0.2% Triton X-100 containing PBS. The following primary antibodies were administered in blocking buffer: mouse anti-Calretinin (Swant; 1:250), chicken anti-Gfp (Aves Labs; 1:500), rabbit anti-Mct8 (Atlas Antibodies; 1:250), mouse anti-Nkx2.1 (Thermo Scientific; 1:100), and mouse anti-Olig2 (Millipore; 1:250). In the same way, Ki67 was visualized on E12.5 sections using a rabbit anti-Ki67 antibody (Abcam, 1:250). For detection of Oatp1c1, fresh-frozen sections and, only in case of costaining with anti-YFP, PFA-fixed sections were treated as described previously (Mayerl et al. 2012). Briefly, sections were fixed for 10 min in Methanol at −20°C and air-dried. Blocking was performed using 1% milk powder in 0.2% Triton X-100 containing PBS for 45 min. Sections were incubated with rabbit anti-Oatp1c1 (kindly provided by Prof. Theo Visser; 1:100) and antibodies as above overnight in blocking buffer. Sections were incubated with secondary antibodies and Hoechst33258 as above and imaged using a Leica SP8 confocal microscope.

In Situ Hybridization

Fresh-frozen cryosections were pretreated as described before (Heuer et al. 2000). In brief, frozen coronal forebrain sections (20 µm) were air-dried, followed by 60 min fixation in a 4% phosphate-buffered paraformaldehyde (PFA) solution (pH 7.4) and permeabilization in 0.4% Triton-X 100 containing PBS for 10 min. Acetylation was carried out in 0.1 M tri-ethanolamine (pH 8.0) containing 0.25% (v/v) acetic anhydride. Sections were dehydrated and covered with hybridization mix.

Third-generation fluorescent ISH experiments (FISH) were performed as described elsewhere (Choi et al. 2018). Probes against Nkx2.1, Ptc1, Shh, and Smo consisting of sets of 20 individual sequences for the target were commercially designed and generated. Probes, buffers, and fluorescently-labeled hairpins were purchased from Molecular Instruments. Slides were incubated with hybridization buffer for 10 min at 37°C before probes in hybridization buffer (0.4 pmol per 100 µL) were applied and hybridization was performed for 24 h at 37°C. Sections were rinsed with probe wash buffer and 5× SSC + 0.1% Tween20 (SSCT). Subsequently, sections were incubated with amplification buffer for 30 min at room temperature. Depending on the probe-specific HCR initiator, specific hairpins h1 and h2 (6 pmol per 100 µL amplification buffer) were separately heat-shocked for 90 s at 95°C and cooled down at room temperature for 30 min. Hairpins were mixed in amplification buffer and applied onto the slides. Signal amplification was performed for 16 h at room temperature. Slides were rinsed in SSCT, incubated 5 min with Hoechst33258 (1:10.000, Invitrogen), rinsed in SSCT and cover-slipped. For imaging, a Leica SP8 confocal microscope was used.

Quantification

For all quantifications, the open source program ImageJ (NIH) was employed. The relative integrated density of GAD67 immunofluorescence signals was calculated by measuring the integrated signal density in the area of the somatosensory cortex and dividing this value by the dimension of the analyzed area. Results were normalized to the respective value obtained by analyzing sections from control animals. To determine numbers of Ki67 positive progenitors in the MGE at E12.5 as well as of neurons expressing Calretinin, GFP, PV, and SST, immunopositive cells were counted and normalized to the dimension of the analyzed area. In all histomorphological studies, 3–4 sections per animal were subjected to quantification.

Shh, Smo, Ptc1, and Nkx2.1-specific FISH signals were quantified in the MGE on 2–3 sections containing the MGE per animal. To account for differently sized areas, mean gray values are presented. Areas devoid of specific signals from the same section were used to calculate background intensities that were subtracted from the values above. Control levels for each time point and probe were set as 1.0.

Statistics

All data represent mean + standard mean error. Statistical significance between control, M/O dfl Cre and M/O dko (Cre)

animals was determined by one-way ANOVA whereas statistical significance between control, Mct8 fl Cre, Oatp1c1 fl Cre, and M/O dfl Cre was assessed by two-way ANOVA followed by Bonferroni post hoc testing. Differences were considered significant when $P < 0.05$ and marked as follows: $^{*}P < 0.05$; $^{**}P < 0.01$; $^{***}P < 0.001$.

Results

Absence of Mct8 in Nkx2.1 Expressing Cells Results in Abnormal TH Levels

Global absence of Mct8 and Mct8/Oatp1c1 in mice results in highly elevated serum T3 concentrations and low serum T4 levels whereas serum TH levels in Oatp1c1 ko mice are unaltered (Trajkovic et al. 2007; Dumitrescu et al. 2006; Mayerl et al. 2014). Here, we analyzed serum TH parameters at postnatal day P12 in conditional TH transporter mutant mice lacking Mct8 and/or Oatp1c1 in Nkx2.1 expressing cells and found a similar abnormal TH profile with decreased serum T4 and elevated serum T3 in Mct8 fl Cre mice as in global M/O dko Cre animals (Figure 1A). Surprisingly, M/O dfl Cre mice exhibit reduced T4 serum levels whereas T3 levels were not affected. In comparison, Oatp1c1 fl Cre mice exhibited unaltered serum TH values at P12. We also determined the TH tissue content in cerebrum samples of P12 animals. In line with our previous studies (Mayerl et al. 2014), M/O dko Cre mice exhibited strongly reduced cerebral T4 and T3 concentrations at P12 indicating a severe state of TH deficiency in the CNS (Figure 1B). In contrast, conditional inactivation of Mct8 alone or in combination with Oatp1c1 in Nkx2.1 expressing cells resulted in slightly reduced forebrain T4 levels in both Mct8 fl Cre and M/O dfl Cre mice. No difference in cerebral T4 content was noted in Oatp1c1 fl Cre animals when compared with controls. Likewise, cerebral T3 tissue concentrations were not altered upon Nkx2.1-Cre-induced inactivation of Mct8 and/or Oatp1c1. Taken together, the loss of Mct8 from Nkx2.1 expressing cells and their progeny leads to a mild hypothyroid situation in the brain that is characterized by a 15% reduction in cerebral T4 levels and no changes in cerebral T3 content.

Determination of body weight revealed no differences between control, M/O dfl Cre and M/O dko Cre mice at P12 whereas at P28, M/O dko Cre males only exhibited a significantly lower weight (Supplementary Figure 1A and B) in accordance with prior observations (Mayerl et al. 2014). These data together with a normal litter size and Mendelian frequency among the offspring argue for an unimpeded general somatic development of the knockout animals during early postnatal life.

Subtype-Specific Alterations in Cortical Interneurons Following Deletion of Mct8/Oatp1c1 in the Nkx2.1 Lineage

Recent data revealed that only upon a combined inactivation of Mct8 and Oatp1c1 a strongly reduced number of PV+ interneurons in the somatosensory cortex can be observed (Mayerl et al. 2014). Nkx2.1 positive progenitors in the MGE give rise to PV+ and SST+ cortical interneurons (Wonders and Anderson 2006). Thus, in order to address the cell-autonomous role of Mct8 and Oatp1c1 on the Nkx2.1 lineage, we analyzed cortical interneuron composition at different postnatal ages in M/O dfl Cre animals. First, to evaluate the neurogenic efficiency of the MGE, we enumerated YFP positive nuclei in the somatosensory cortex at P12 and P28 (Supplementary Figure 2A). No differences were found between control, M/O dfl Cre, and M/O dko Cre animals arguing for an unimpeded overall neurogenesis from the Nkx2.1 lineage.

Staining for the interneuron subtype-specific marker PV in the same area, however, disclosed its virtual absence in M/O dfl Cre and M/O dko Cre animals at P12 (Figure 2). Interestingly, deletion of Mct8 alone (as in Mct8 fl Cre mice) did not alter PV interneuron numbers at P12 whereas Oatp1c1 fl Cre exhibited reduced numbers though less severe when compared with M/O dfl Cre animals (Supplementary Figure 2B). PV+ cell numbers increased quickly over time in the somatosensory cortex of M/O dfl Cre mice, reached control levels by P16 and were thereafter indistinguishable from control littermates (Figure 2). The appearance of PV+ interneurons was found to be delayed even further in M/O dko Cre mice since the first pronounced PV staining could only be detected at P21. In these animals, PV+ cell counts remained low and were reduced by more than 50% at P28 compared with control and M/O dfl Cre mice.

Though SST+ interneurons are derived from the same region of the embryonic brain like PV+ interneurons, their density was unaltered in M/O dfl Cre animals at P12, P14, and P28 (Figure 3A). In contrast, SST+ interneuron numbers were consistently almost 3-fold increased in M/O dko Cre animals.

CR+ interneurons are born in the CGE and their generation does not depend on Nkx2.1. Visualizing CR+ cells in the somatosensory cortex revealed scattered cells as well as a strongly immunopositive band underneath the barrel fields that contains cluster of densely packed cells (Figure 3B). At P12, significantly more CR+ cells were found in both M/O dfl Cre and M/O dko Cre mice compared with control animals. With ongoing maturation of the brain, CR+ numbers were reduced in all genotypes. Interestingly, following a strong drop in their cell numbers, no differences were seen in M/O dfl Cre mice at P14 when compared with controls. This decrease was delayed in M/O dko Cre mice and differences disappeared only at P28.

Finally, to evaluate the general state of inhibition in the somatosensory cortex, we analyzed the expression of the pan-GABAergic marker and GABA producing enzyme Glutamate decarboxylase (Gad) 67 (Figure 3C). As reported before, Gad67 immunopositive signals appeared later in M/O dko Cre mice when compared with controls (Mayerl et al. 2014). Likewise, Gad67 integrated density was decreased in M/O dko Cre animals at all investigated time points. In M/O dfl Cre mice, signal intensities appeared to be reduced in comparison to control littermates though statistical significance was not reached. However, Gad67 expression was visibly more pronounced in M/O dfl Cre mice than in M/O dko Cre animals. Together, our findings indicate permanent alterations and transient delays in the maturation of the GABAergic system in M/O dko Cre and M/O dfl Cre mice, respectively. Moreover, our data point to at least 2 different mechanisms in interneuron neurogenesis that depend on proper TH transport by Mct8 and Oatp1c1.

Shh Signaling is Impaired Upon Global Loss of Mct8 and Oatp1c1

One of the most critical steps in the development of interneurons is their specification that takes place in the ganglionic eminences before the onset of migration and is governed by a variety of morphogens such as Shh (Kelsom and Lu 2013). In the canonical signaling pathway, binding of soluble Shh to its receptor Patched (Ptc) on the surface of target cells releases the Ptc-mediated block of Smoothened (Smo) (Carballo et al. 2018). Smo then activates Gli transcription factors that translocate

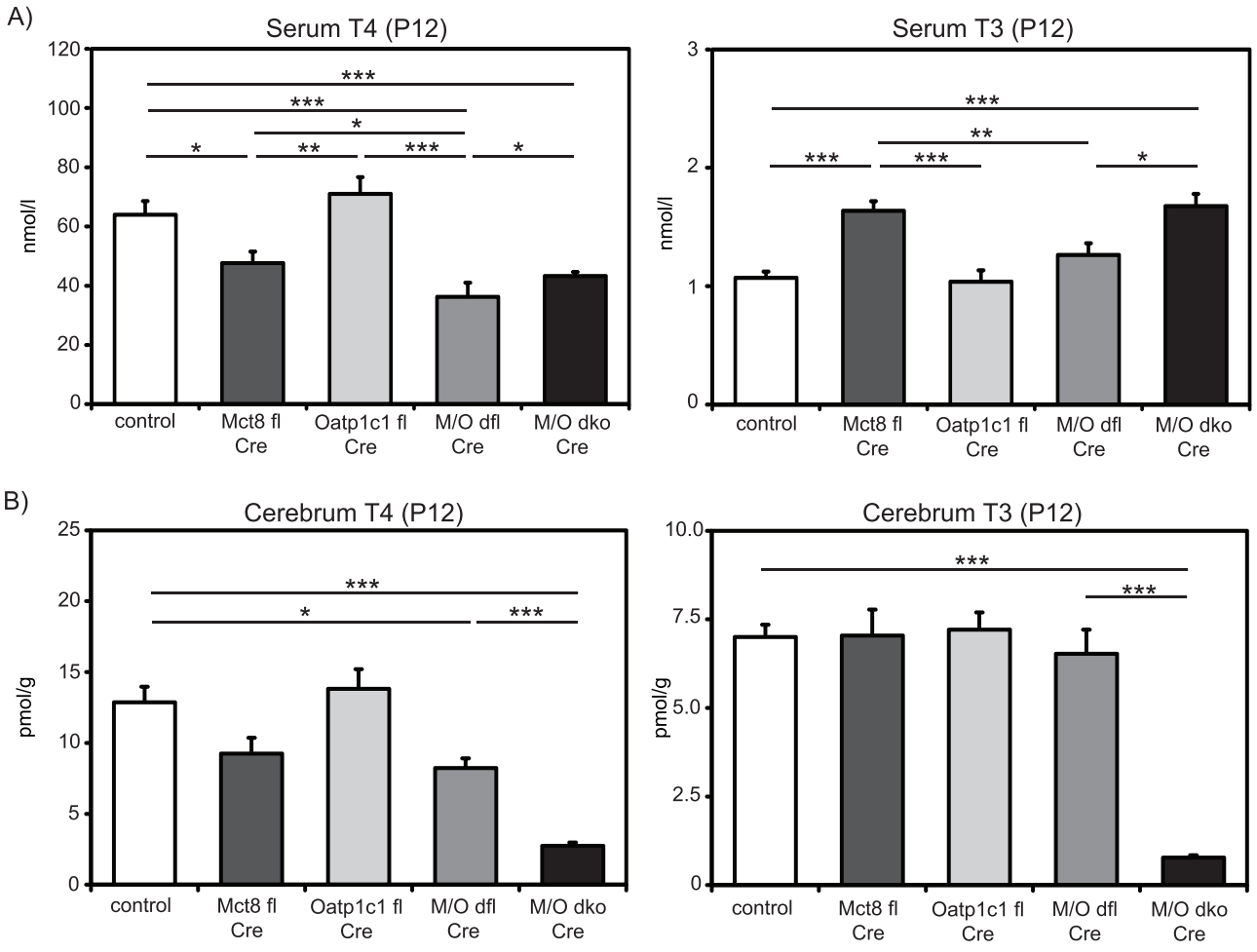

Figure 1. Evaluation of TH levels: (A) Serum TH was analyzed at P12 and revealed decreased T4 levels and increased T3 concentrations in Nkx2.1-Cre positive Mct8 fl, M/O dfl, and M/O dko mice. $n = 3$ (Mct8 fl Cre); $n = 6$ (Oatp1c1 fl Cre); $n = 7$ (control, M/O dfl Cre, M/O dko Cre). (B) Total forebrain T4 levels were mildly reduced in Mct8 fl Cre and M/O dfl Cre animals at P12, whereas T3 content was not altered. M/O dko Cre presented strongly reduced T4 and T3 values. n = 7 (control); $n = 8$ (Mct8 fl Cre, Oatp1c1 fl Cre); $n = 10$ (M/O dko Cre). $^{*}P < 0.05$, $^{**}P < 0.01$, $^{***}P < 0.001$.

into the nucleus and activate expression of target genes. In the MGE, Shh signaling is crucial for PV interneuron identity via the maintenance of Nkx2.1 (Xu, Wonders, and Anderson 2005).

As Shh signaling components themselves are well-known TH target genes (Desouza et al. 2011), we addressed their expression in the MGE of TH transporter deficient mice at E12.5 using third-generation FISH experiments (Figure 4). In agreement with previous results, we detected prominent Shh transcript expression in the mantle zone of the MGE (Figure 4A) (Desouza et al. 2011). Quantification of Shh-specific signals revealed unaltered transcript levels in M/O dfl Cre animals whereas Mct8/Oatp1c1 dko mice presented a strong, 50% reduction in Shh mRNA expression. Likewise, transcript levels of the Shh receptor Smo were significantly reduced in the MGE ventricular zone in Mct8/Oatp1c1 dko animals only (Figure 4B). Ptc1 mRNA levels were not different between the groups when quantified over the total length of the ventricular zone (Supplementary Figure 3). However, and in agreement with visually discernible regional differences, we found significantly reduced Ptc1 transcript levels in M/O dko mice when quantified in the ventral half of the MGE only (Figure 4C). These reductions in Shh signaling components were accompanied by decreased levels of Nkx2.1 mRNA in the ventricular and subventricular zones of the MGE in M/O dko animals, but not in the conditional knockout model (Figure 4D). In contrast, proliferation of MGE progenitors as determined by density of Ki67+ nuclei was not affected in the different knockout models (Supplementary Figure 3B). Together, our results indicate that absence of Mct8 and Oatp1c1 interferes with proper interneuron specification in the MGE via modulation of Shh signaling in a noncell-autonomous manner.

Mct8 and Oatp1c1 Are Not Expressed in MGE Progenitors at E12.5

The discrepancy between the cell-autonomous effects of Mct8 and Oatp1c1 on the appearance of PV immunoreactivity in the postnatal somatosensory cortex and the only noncell-autonomous requirement of both TH transporters for Shh signaling in the MGE prompted us to investigate their expression pattern in more detail. At E12.5, the MGE of control mice as identified by its characteristic expression of Nkx2.1 was devoid of any Mct8-specific staining (Figure 5A). We observed, however, strong Mct8 immunopositivity in the area of the dorsal midline on the same sections (Figure 5B). Here, Mct8 protein is restricted

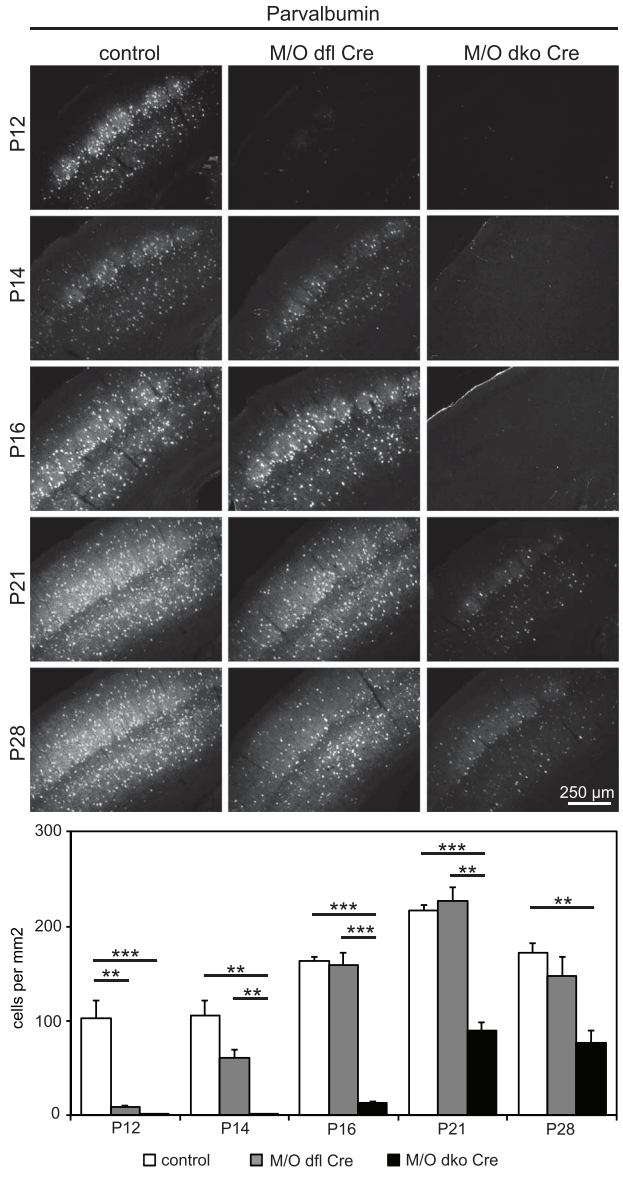

Figure 2. Specific alterations in cortical PV+ interneurons: PV immunoreactivity was assessed in the somatosensory cortex at different postnatal time points. At P12, M/O dfl Cre mice and M/O dko Cre mice were almost devoid of PV+ interneurons. PV+ cell numbers increased in M/O dfl Cre mice at P14 and reached control levels at P16. M/O dko Cre mice presented with a further delayed appearance of PV+ interneurons that was first clearly noticed at P21 as well as persistently reduced PV+ cell numbers. $n = 5$ (M/O dko Cre at P12; control at P14); $n = 4$ (M/O dko Cre at P14 and P21); $n = 3$ (all other groups). $^{**}P < 0.01$, $^{***}P < 0.001$.

to a region that is invaginating into the lateral ventricle, an area known to give rise to the choroid plexus (Johansson 2014). Likewise, Oatp1c1 protein was not observed in Nkx2.1 positive MGE progenitor cells (Figure 5C). Oatp1c1 immunoreactivity was rather present in what appears to be ependymal structures along the dorsal and ventral ventricular borders between the MGE and LGE as well as MGE and septum, respectively. A similar staining pattern was found in the dorsal midline region with Oatp1c1 localizing to putative ependymal structures along the border of the developing cortex with both the ventricular and subarachnoid spaces (Figure 5D). These expression patterns point to unique roles of both TH transporters at embryonic brain barriers and a complex and precisely regulated TH supply to the E12.5 brain.

Mct8 and Oatp1c1 Are Expressed in Interneurons at Later Developmental Stages

We wondered if, despite their absence from progenitor cells in the MGE, Mct8 and Oatp1c1 are present in interneurons at a later developmental stage. Thus, we subjected brain sections obtained at different embryonic and postnatal time points to immunostaining. In Wt mice at E14.5, E18.5, and P0, strong Mct8 immunoreactivity was consistently observed in the choroid plexus only (Figure 6A–C, respectively) whereas Oatp1c1 protein was detected in the choroid plexus and elongated structures in different brain areas that are characteristic of blood vessels (Figure 6D–F). Moreover, a few distinct Oatp1c1 positive cells could be seen in the P0 cerebral cortex (Figure 6F) prompting us to investigate whether these are of interneuronal identity. Given the absence of specific markers for migrating interneurons, we reverted to Mct8 wt; Oatp1c1 wt; Nkx2.1-Cre; EYFP control mice and analyzed coexpression of TH transporters and YFP as an indicator for their MGE-derived origin (Figure 6G and H). We found YFP+ cells in all brain areas such as cerebral cortex, striatum, or hypothalamus (Supplementary Figure 4). Mct8 immunopositive signals were not detectable in the vast majority of YFP+ cells in these areas, only a few exceptions were found, for example in the hypothalamus (Supplementary Figure 4A). Likewise, no Oatp1c1 coexpression was observed in most of the YFP+ cells throughout the brain (Supplementary Figure 4B) with the exception of the cerebral cortex where we found occasionally strong Oatp1c1 immunofluorescence signals in YFP+ cells. To exclude that these cells represent oligodendroglia lineage cells originating from Nkx2.1-expressing cells in the preoptic area that will be YFP+ as well, we further included Olig2 as a marker and focused on Olig2 negative cells. At P0, YFP+/Olig2- cells did not show coexpression of Mct8 (Figure 6H). Oatp1c1 protein, however, was seen in YFP+/Olig2- cells indicative of MGE-derived interneurons. No such Oatp1c1+ interneurons were detectable in M/O dfl Cre mice at P0 (Supplementary Figure 5A). Intriguingly, upon maturation, the expression pattern of TH transporters changes: We noticed expression of Mct8 in PV+ cell protrusions and occasionally in the PV+ soma of P12 control mice (Figure 6I) that was absent in M/O dfl Cre mice (Supplementary Figure 5B). In contrast, CR+ cell bodies and protrusions were devoid of Mct8+ signals (Supplementary Figure 5C). Oatp1c1 immunoreactivity was neither visible in PV+ nor CR+ interneurons at P12 (Figure 6K and Supplementary Figure 5D, respectively). Our results highlight in sum a spatially and temporally fine-tuned expression of TH transporters in interneurons that may underlie their exceptional TH sensitivity and which may account for the observed cell-autonomous effects seen in M/O dfl Cre animals, for example on PV+ cell numbers.

Discussion

Proper brain development depends on the timed availability of TH as TH regulates proliferation, migration, and differentiation of neural precursor cells (Bernal 2005). One example of such a critical TH-dependent process is the generation of inhibitory GABAergic interneurons. Particularly, a subtype of interneurons positive for the Calcium binding protein PV is

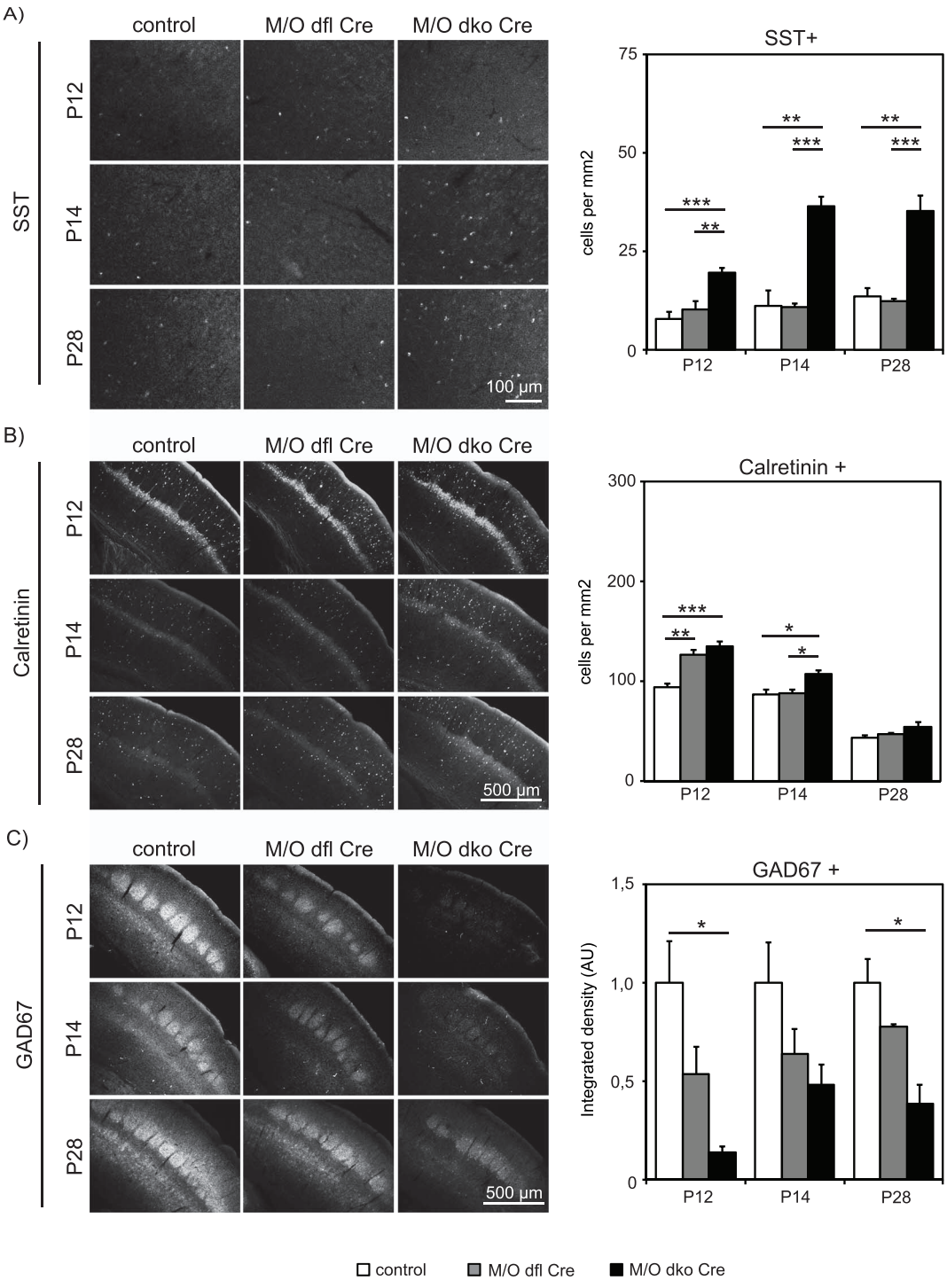

Figure 3. Consequences of TH transporter deficiency on the cortical inhibitory system: (A) SST immunoreactivity was evaluated in the somatosensory cortex. At all indicated time points, number of SST+ cells was unaltered in M/O dfl Cre mice, but elevated in M/O dko animals. (B) Sections were stained for CR and immunopositive cell bodies were enumerated. At P12, M/O dfl Cre and M/O dko Cre mice exhibited a higher density of CR+ interneurons. Differences disappeared first in M/O dfl Cre mice at P14 and in M/O dko Cre mice at P28. (C) The general GABAergic marker Gad67 was visualized and Gad67 integrated density was determined. Gad67 levels were reduced slightly in M/O dfl Cre mice and strongly in M/O dko animals. Differences were present at all analyzed time points. $n = 5$ (M/O dko-Cre at P12; control at P14); $n = 4$ (M/O dko-Cre at P14); $n = 3$ (all other groups). $^{*}P < 0.05$, $^{**}P < 0.01$, $^{***}P < 0.001$.

especially sensitive toward alterations in TH signaling. TH insufficiency during brain development has been shown to decrease the number of PV positive interneurons encompassing basket and chandelier cells in the rat cerebral cortex (Berbel et al. 1996; Gilbert et al. 2007). A similar observation was made in mouse mutants globally expressing a dominant negative form of TRα1

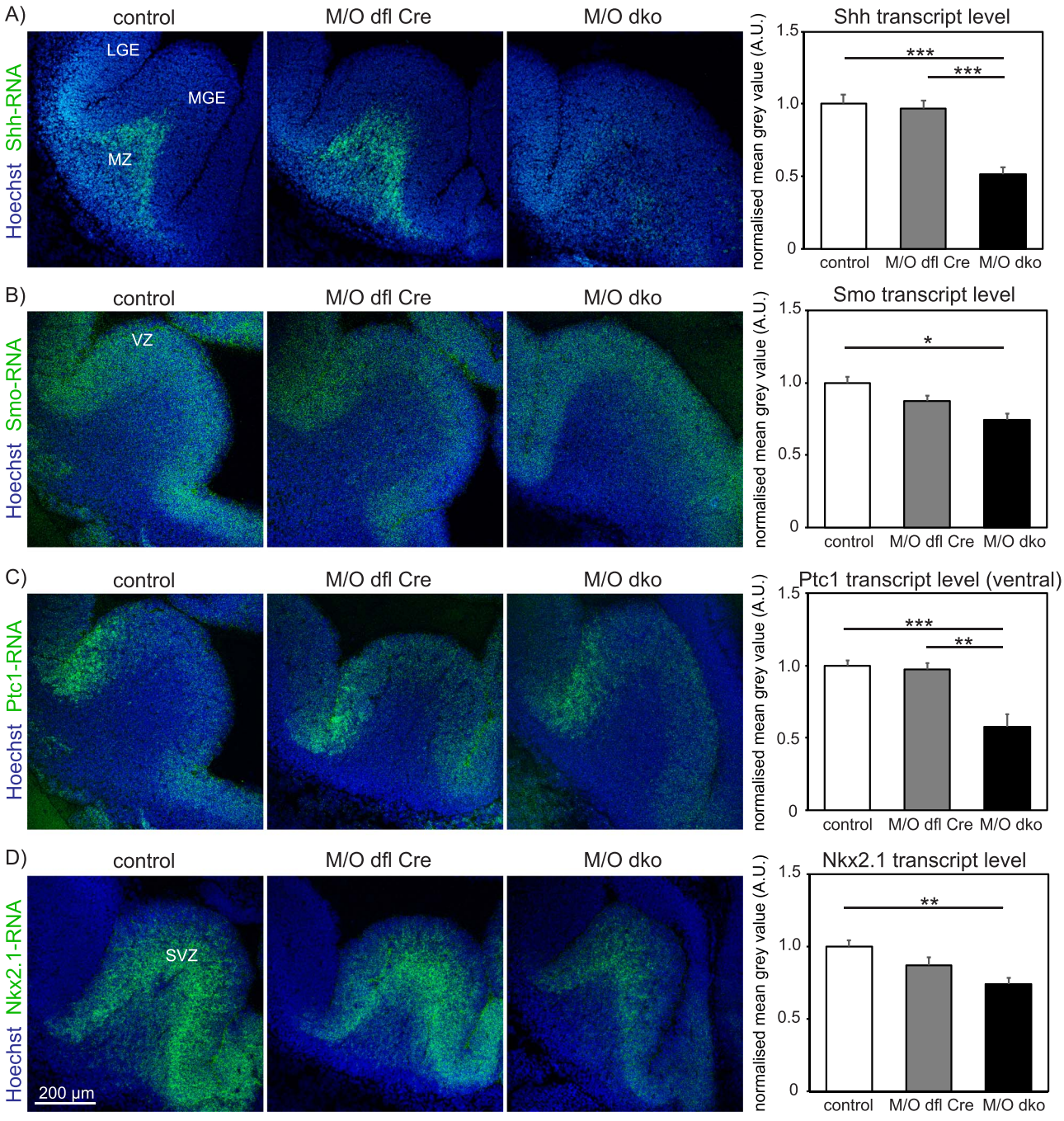

Figure 4. TH transporter deletion affects Shh signaling: Cryosections from E12.5 embryonic brains were subjected to fluorescence in situ hybridization. Transcript-specific expression is shown in green whereas Hoechst33258-counterstained nuclei appear blue. (A) Shh transcript-specific signals were detected in the mantle zone (MZ) of the MGE. Expression levels were comparable between control and M/O dfl Cre mice, but reduced in M/O dko animals. (B) Smo mRNA is expressed in the ventricular zone (VZ) of the MGE. Only M/O dko mice demonstrated significantly reduced Smo transcript levels. (C) Expression of Ptc1 mRNA in the MGE ventricular zone exhibiting subregional differences with stronger signal intensities at the borders to the septum (ventral) and LGE (dorsal). Although Ptc1 levels seemed unaltered in the dorsal part, a decrease was observed in the ventral area of M/O dko mice only. (D) Nkx2.1 mRNA distribution in the MGE. Although present in the ventricular and mantle zones, highest expression levels are found in the subventricular zone (SVZ). Total transcript expression was reduced in M/O dko mice only. $n = 6$ (control); $n = 5$ (M/O dfl Cre and M/O dko). $^{*}P < 0.05$, $^{**}P < 0.01$, $^{***}P < 0.001$.

that leads to a delayed appearance of cortical PV interneurons (Wallis et al. 2008). Likewise, Mct8/Oatp1c1 dko mice, a mouse model of AHDS, which exhibit severely reduced central TH concentrations, display permanently reduced PV interneuron numbers in the somatosensory cortex (Mayerl et al. 2014). That this holds true for human brain development as well was confirmed on post mortem CNS sections of AHDS patients, which presented a decreased PV immunoreactivity in the cerebral cortex (Lopez-Espindola et al. 2014). Nonetheless, the key question as to whether perturbations in PV interneuron generation in AHDS

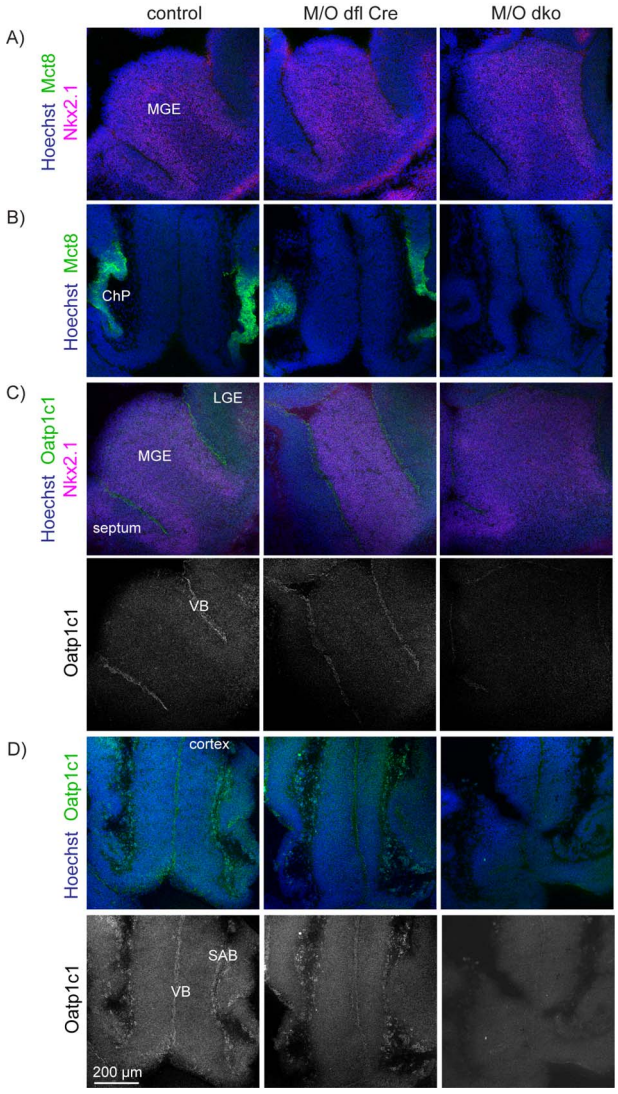

Figure 5. TH transporter expression in the embryonic brain: Immunofluorescent analysis of TH transporter expression at E12.5 conducted on fresh-frozen cryosections (A) Mct8 (green) protein is not expressed in the MGE identified by Nkx2.1 immunoreactivity (pink). (B) Expression of Mct8 (green) in restricted, invaginated areas along the dorsal midline forming into the choroid plexus (ChP) in control and M/O dfl Cre animals. Mct8-specific staining was absent in M/O dko mice. (C) Oatp1c1 protein (green in merge, and single b/w channel) was found along the ventricular border (VB) between the MGE and LGE as well as MGE and septum, but was undetectable in Nkx2.1 (pink) expressing cells in the MGE of control and M/O dfl Cre mice. No specific staining was observed in M/O dko animals. (D) Localization of Oatp1c1 protein (green in merge, and single b/w channel) along the ventricular border (VB) of the dorsal midline region and subarachnoid border (SAB) region. Oatp1c1-specific signals were seen only in control and M/O dfl Cre, but not M/O dko mice. In all images, Hoechst33258 counterstained nuclei are depicted in blue.

result from a general TH deficiency in the CNS due to a loss of TH transport across brain barriers or whether MCT8 exerts additionally a cell-autonomous function in providing interneuronal progenitors with TH remains elusive. Unraveling the cell-specific action of MCT8 is of profound relevance for the development of AHDS treatment strategies as such an approach does not only define the respective neural target cells but also discloses the therapeutic window for any successful intervention (such as application of the TH analogue Triac) (Groeneweg et al. 2019).

Here, we describe our strategy to resolve this important question by taking advantage of Mct8/Oatp1c1 dko mice and comparing them to a conditional knockout model in which both genes encoding the 2 transporters are inactivated (by deletion of exon 3) in a subset of interneuron progenitors and, consequently, also in their progeny. To this end, we utilized mice expressing Cre recombinase under the Nkx2.1 promotor, a key transcription factor in the generation of MGE-derived PV+ and SST+ interneurons. We studied the subset composition of GABAergic interneurons by immunohistochemistry at different postnatal time points and found a transient reduction in the number of cortical PV interneurons in the conditional M/O dfl Cre model. As a caveat of using Nkx2.1 Cre mice we also achieved a deletion of Mct8 in the thyroid gland causing decreased thyroidal T4 secretion (Di Cosmo et al. 2010; Trajkovic-Arsic et al. 2010) which in turn leads to significantly reduced serum T4 levels and slightly reduced forebrain T4 content (Figure 1A and B). One might therefore argue that the mild hypothyroid situation present in the M/O dfl Cre cerebrum at P12 causes the observed alterations in PV+ immunoreactivity. However, neither global Mct8 ko nor Oatp1c1 ko mice which both exhibit even lower cerebral T4 concentrations show such a remarkable reduction in PV+ cell number at P12 as seen in M/O dfl Cre mice (Mayerl et al. 2014). In addition, PV+ cell density was unaltered in Mct8 fl Cre mice despite exhibiting similar peripheral and central TH levels like M/O dfl Cre animals. This further argues against the possibility that an altered thyroidal state due to our Nkx2.1-Cre mediated knockout strategy influences interneuron neurogenesis. Along this line, results from Oatp1c1 fl Cre mice that though presenting a euthyroid cerebrum exhibit strongly reduced cortical PV+ cell numbers indicate that cellular, rather than overall cerebral TH levels are critical for interneuronal migration/maturation events.

To ensure proper TH supply to late-stage developing interneurons, expression of both Mct8 and Oatp1c1 is required as evidenced by the more severe reduction in PV+ cell numbers in M/O dfl Cre mice compared with the single mutants Mct8 fl Cre and Oatp1c1 fl Cre mice, respectively. The presence of Mct8 in PV+ but not in CR- interneurons certainly contributes to the differences in TH sensitivity of both subtypes. Thus, cell-autonomous Mct8 and Oatp1c1 expression impacts the maturation of the cortical GABAergic system. Additionally, both transporters seem to harbor a second, noncell-autonomous role in early interneuron development by presumably controlling TH flux across different brain barriers thereby also influencing PV neuron neurogenesis.

That intracellular TH signaling in GABAergic neurons and/or their progenitors is indeed mandatory for proper maturation of PV neurons was recently demonstrated by Richard et al. (2020) who introduced a dominant negative mutation in the TH receptor TRα1 into all GABAergic interneurons and their progenitors. For that purpose, they took advantage of a Gad2 Cre mouse and observed a reduction in the number of PV interneurons at P14 thereby confirming a cell-autonomous role of TRα1. Unfortunately, they were unable to assess whether PV immunoreactivity would normalize at later time points as seen in M/O dfl Cre animals since TRa1 mutant mice were prone to lethal epileptic seizures. Whether an elimination of both TH transporters Mct8 and Oatp1c1 in all GABAergic neurons would lead to seizures as well has not been addressed yet. Of note, epileptic seizures are a known pathology of AHDS patients (Groeneweg et al. 2020) and

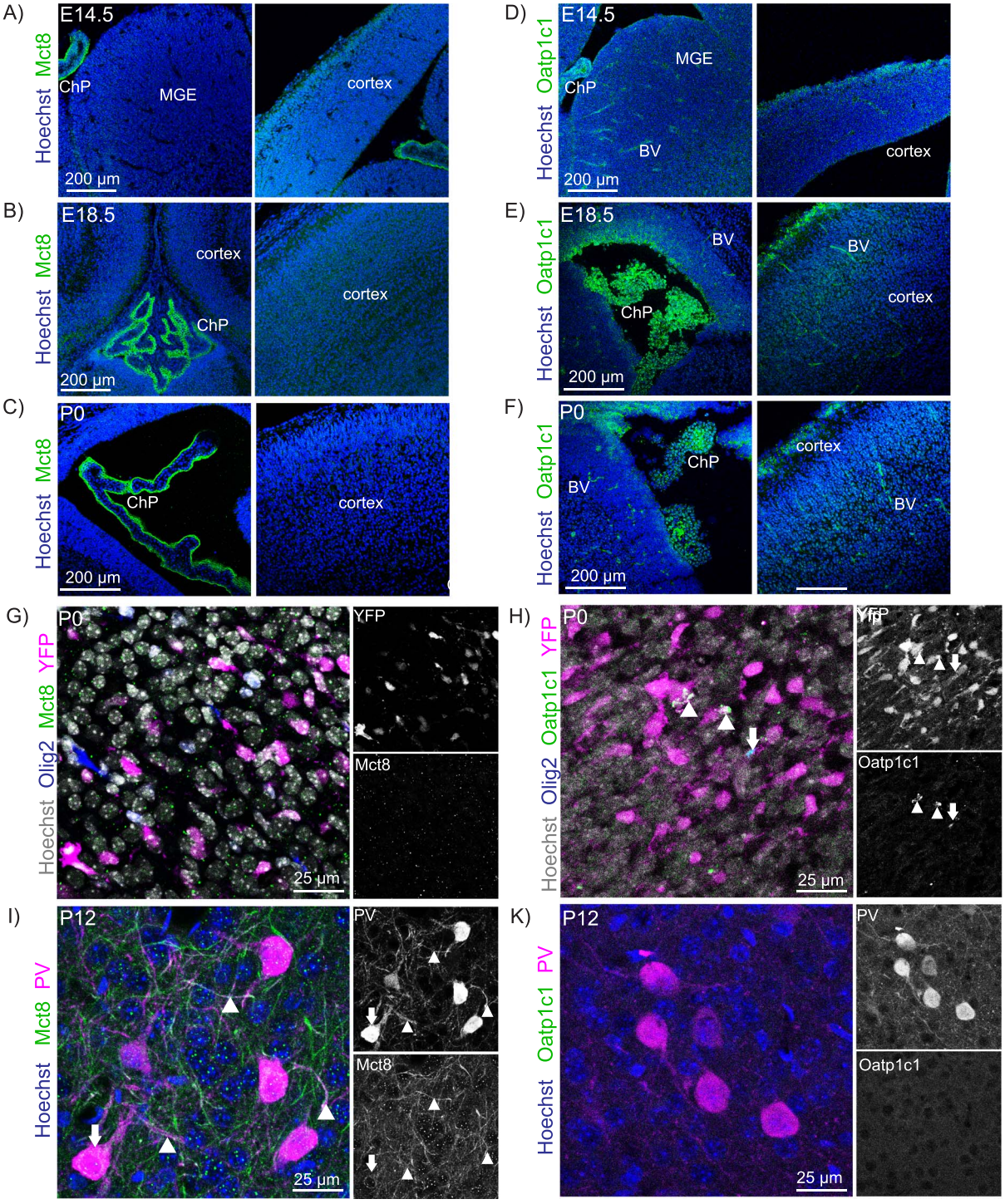

Figure 6. TH transporter expression throughout embryonic and early postnatal development: Immuno-fluorescent analysis of TH transporter expression. In Wt mice, Mct8 (green) protein is detectable in choroid plexus (ChP) structures, but not in the MGE or cerebral cortex at (A) E14.5, (B) E18.5, and (C) P0. Oatp1c1 protein (green) is present in ChP and blood vessel (BV) like structures in brain regions such as the cerebral cortex at (D) E14.5, (E) E18.5, and (F) P0. (G) Control mice expressing Nkx2.1-Cre and YFP transgenes do not exhibit Mct8 immunopositive signals (green) in YFP+ (magenta)/Olig2- (blue) interneurons in the somatosensory cortex at P0. Merge picture and single Mct8 and YFP channels are shown. (H) Oatp1c1 protein (green) is present in distinct, few YFP (magenta) positive either Olig2 (blue) negative cells (i.e., interneurons; arrowheads) or Olig2 positive cells (i.e., oligodendroglia cells; arrow) at P0 in the somatosensory cortex of control mice. Merge picture and single Mct8 and YFP channels are shown. (I) In control mice at P12, Mct8 (green) protein is visible in PV+ (magenta) cell bodies (arrow) and cell protrusions (arrowheads) in the somatosensory cortex. (K) Oatp1c1 protein (green) is not observed in PV+ (magenta) structures in the P12 somatosensory cortex of control mice. Hoechst33258 counterstained nuclei are depicted in blue (A–F, I, and K) or gray (G and H).

may well be related to a cell-intrinsic loss of MCT8 function in interneuron precursor cells.

Apart from PV+ cells, other cortical GABAergic interneurons require TH signaling for proper maturation as well. Numbers of SST+ cells are increased in a growth-retarded hypothyroid mouse strain and in mice expressing a dominant negative form of TRα1 in GABAergic interneurons only (Uchida et al. 2014; Richard et al. 2020). In line with these findings, M/O dko mice exhibit a 3-fold increase in SST neuron density that is most likely a consequence of the general TH deficient state in the CNS. Importantly, though our conditional knockout strategy also eliminates Mct8/Oatp1c1 expression in SST interneurons, we could not detect any alterations in cortical SST+ cell numbers in M/O dfl Cre mice. Altogether, these data clearly indicate that TH signaling is cell-intrinsically required in SST+ cells but the uptake of TH into this type of inhibitory neurons is not dependent on Mct8 and Oatp1c1. Which alternative transporters may facilitate access to these neurons has not been clarified yet. Although a wealth of putative TH-transporting proteins has been identified in in vitro studies (Groeneweg et al. 2020), very limited information is currently available regarding their spatiotemporal expression pattern and, even more importantly, regarding their pathophysiological role in cellular TH transport. It is, however, very likely that the generation and characterization of new animal models will unravel novel TH transporter candidates important for proper brain development and function.

A third subtype of GABAergic interneurons that is affected by global Mct8/Oatp1c1 deficiency are CR interneurons. In line with previous observations, we detected more CR positive neurons in the somatosensory cortex of the global M/O dko mouse model (Mayerl et al. 2014). This is in agreement with the situation in mice harboring a dominant negative form of TRα1 (Wallis et al. 2008). In contrast, M/O dfl Cre animals exhibited transiently elevated CR numbers at P12 only. This is a rather surprising finding as the generation of CGE-derived CR interneurons is independent of Nkx2.1 and, therefore, will not be targeted by our conditional knockout strategy. The results from both Mct8/Oatp1c1 deficient animal models point to a fate shift during interneuron specification in the MGE. Such a fate shift has already been observed upon removal of Nkx2.1 during embryonic development that in turn has led to an increase in CR+ at the expense of PV+ interneurons (Butt et al. 2005). Likewise, inhibition of Shh signaling was shown to reduce Nkx2.1 expression and consecutively induce a fate shift in interneuron identity characterized by the conversion of PV+ and SST+ neurons to CR interneurons that normally originate from the CGE (Xu, Wonders, and Anderson 2005; Xu et al. 2010). Whether this fate shift is sufficient to fully explain the reductions in PV+ interneuron numbers or whether PV+ neurons simply cannot be detected because TH may regulate the expression of this marker protein as suggested by (Gilbert et al. 2007) remains elusive. The latter hypothesis may be tested in future studies using PV-Cre mice. Our data on equal YFP+ cell numbers, altered subtype composition in the postnatal cortex, and TH transporter expression in interneuronal subtypes, however, argues for a combination of both possibilities.

To unravel a mechanism by which a fate shift might be induced in our TH transporter mouse mutants, we studied the expression of key Shh signaling components in the MGE at E12.5. In agreement with previous work (Nery, Wichterle, and Fishell 2001), we detected pronounced Shh transcript expression in the mantle zone of M/O dfl Cre mice and control littermates whereas Shh-specific FISH signals were found to be reduced to 50% in M/O dko animals only. Similarly, expression of Shh receptors Ptc1 and Smo in the MGE ventricular zone (Rallu et al. 2002) was significantly impaired in M/O dko mice only. As Shh signaling maintains Nkx2.1 expression in the MGE (Xu, Wonders, and Anderson 2005), it was not too surprising that Nkx2.1 mRNA expression was also found to be compromised in M/O dko mice only. Consequently, the impaired Shh/Nkx2.1 pathway may underpin the permanent fate shift of MGE-derived interneurons that is visible only in the M/O dko model.

How does the absence of Mct8/Oatp1c1 initiate this fate shift? All 3 analyzed Shh signaling components (Shh, Ptc1, Smo) are positively TH-regulated genes (Desouza et al. 2011). The reduced expression of these genes suggests that the E12.5 M/O dko embryonic brain, but not that of M/O dfl Cre mice, is already in a TH deficient situation. This hypothesis is substantiated by our immunostaining experiments revealing the presence of Mct8 and Oatp1c1 at different brain barriers but not in progenitor cells within the MGE. Thus, in M/O dko mice, TH transport across brain barriers might already be compromised during embryonic stages which in turn exerts secondary, noncell-autonomous effects on interneuron neurogenesis (Supplementary Figure 6).

Based on the time-shifted expression of Oatp1c1 in YFP+ cells at P0 and then Mct8 in PV+ interneurons at P12, we further postulate that both TH transporter adopt a cell-autonomous role in interneurons at a later developmental stage (Supplementary Figure 6). Their absence then might interfere with proper migration or network integration which may explain the delayed appearance of PV interneurons in the M/O dfl Cre mouse. In agreement with this sequential TH transporter expression profile, our analysis of PV+ cell numbers in Oatp1c1 fl Cre and Mct8 fl Cre mice highlights a more prominent role of Oatp1c1 in regulating interneuron migration and/or maturation though the underlying mechanistic alterations remain elusive. The possibility that abolished Mct8 expression in PV+ interneurons interferes with cellular functions such as electrophysiological properties needs to be explored further. The theory of a late-stage cell-autonomous impact is in accordance with recent results in mice in which all interneurons express a dominant negative form of TRα1 and in which cell-autonomous TRα1 signaling was found to govern late steps of the development of several classes of GABAergic interneurons (Richard et al. 2020).

Our results are in line with recent, elegant studies on the role of MCT8 during neurogenesis in the chicken embryo. Knockdown of MCT8 in Purkinje cells by MCT8-RNAi vector electroporation during early development resulted in both cell-autonomous and noncell-autonomous effects on cerebellar development such as granule cell proliferation and migration deficits (Delbaere et al. 2017). Using a similar approach, Vancamp et al. (2017) abolished MCT8 expression in the developing chicken optic tectum and found a drastically impaired generation of both glutamatergic and GABAergic neurons. The striking resemblance between these reports and our data on MGE-derived interneurons in the mouse highlights the critical need for proper TH transport already during early stages of brain development.

Of note, the MGE does not only give rise to interneurons, but together with the anterior entopeduncular area/preoptic also to the first wave of oligodendrocyte progenitor cells (OPC) (Kessaris et al. 2006). These first wave OPCs are generated from Nkx2.1 positive progenitors around E12.5, migrate through the entire telencephalon and enter the developing cortex around E16. In light of the reduced MGE Nkx2.1 levels in M/O dko animals it

remains to be determined whether this first wave of OPCs is compromised and whether such as scenario contributes to the apparent hypomyelination phenotype of M/O dko mice and even AHDS patients (Mayerl et al. 2014; Lopez-Espindola et al. 2014).

Together, our results reveal a hitherto unknown early function of TH transporters Mct8 and Oatp1c1 in the E12.5 embryonic brain and a complex cell-autonomous as well as noncell-autonomous impact of both proteins on the generation of interneurons. Both transporters act in concert to facilitate the proper TH supply to the developing brain and developing interneurons that will be ultimately important for a balanced excitation/inhibition in the cerebral cortex. Understanding the spatiotemporal regulation of TH transport is not only instrumental for an adequate therapy for AHDS, but may enable us to harness the potential of TH to aid interneuron neurogenesis in other disorders as well.

Supplementary Material

Supplementary material can be found at *Cerebral Cortex* online.

Funding

German Research Foundation (DFG) (MA7212/2-1; MA7212/2-2; HE3418/8-2; CRC/TR296-P01, CRC/TR296-P09, CRC/TR296-P19), the Federal Ministry of Education and Research (BMBF; 01GM1401) and Sherman Family.

Notes

We are grateful to Markus Korkowski and Natalie Sadowski as well as to the FLI and UK Essen animal facility staff for their valuable help and excellent work. Furthermore, we thank Dr Anthony Squire and Alexandra Brenzel (Imaging Center Essen) for their invaluable support. *Conflict of Interest*: None declared.

Authors' contributions

SM and HH devised the experiments and wrote the manuscript. SM, JC, and ES performed experiments and conducted the analysis. AB determined serum TH levels and VMD measured TH tissue concentrations.

References

Berbel P, Marco P, Cerezo JR, DeFelipe J. 1996. Distribution of parvalbumin immunoreactivity in the neocortex of hypothyroid adult rats. *Neurosci Lett*. 204:65–68.

Bernal J. 2005. Thyroid hormones and brain development. *Vitam Horm*. 71:95–122.

Butt SJ, Fuccillo M, Nery S, Noctor S, Kriegstein A, Corbin JG, Fishell G. 2005. The temporal and spatial origins of cortical interneurons predict their physiological subtype. *Neuron*. 48:591–604.

Carballo GB, Honorato JR, de Lopes GPF, Spohr TCLDE. 2018. A highlight on Sonic hedgehog pathway. *Cell Commun Signaling*. 16:11.

Choi HMT, Schwarzkopf M, Fornace ME, Acharya A, Artavanis G, Stegmaier J, Cunha A, Pierce NA. 2018. Third-generation in situ hybridization chain reaction: multiplexed, quantitative, sensitive, versatile, robust. *Development*. 145:dev165753.

de Vries EM, Nagel S, Haenold R, Sundaram SM, Pfrieger FW, Fliers E, Heuer H, Boelen A. 2016. The role of Hypothalamic NF-kappaB signaling in the response of the HPT-axis to acute inflammation in female mice. *Endocrinology*. 157:2947–2956.

Delbaere J, Vancamp P, Van Herck SL, Bourgeois NM, Green MJ, Wingate RJ, Darras VM. 2017. MCT8 deficiency in Purkinje cells disrupts embryonic chicken cerebellar development. *J Endocrinol*. 232:259–272.

Desouza LA, Sathanoori M, Kapoor R, Rajadhyaksha N, Gonzalez LE, Kottmann AH, Tole S, Vaidya VA. 2011. Thyroid hormone regulates the expression of the sonic hedgehog signaling pathway in the embryonic and adult Mammalian brain. *Endocrinology*. 152:1989–2000.

Di Cosmo C, Liao XH, Dumitrescu AM, Philp NJ, Weiss RE, Refetoff S. 2010. Mice deficient in MCT8 reveal a mechanism regulating thyroid hormone secretion. *J Clin Invest*. 120:3377–3388.

Dumitrescu AM, Liao XH, Best TB, Brockmann K, Refetoff S. 2004. A novel syndrome combining thyroid and neurological abnormalities is associated with mutations in a monocarboxylate transporter gene. *Am J Hum Genet*. 74:168–175.

Dumitrescu AM, Liao XH, Weiss RE, Millen K, Refetoff S. 2006. Tissue-specific thyroid hormone deprivation and excess in monocarboxylate transporter (mct) 8-deficient mice. *Endocrinology*. 147:4036–4043.

Friesema EC, Grueters A, Biebermann H, Krude H, von Moers A, Reeser M, Barrett TG, Mancilla EE, Svensson J, Kester MH *et al*. 2004. Association between mutations in a thyroid hormone transporter and severe X-linked psychomotor retardation. *Lancet*. 364:1435–1437.

Gilbert ME, Sui L, Walker MJ, Anderson W, Thomas S, Smoller SN, Schon JP, Phani S, Goodman JH. 2007. Thyroid hormone insufficiency during brain development reduces parvalbumin immunoreactivity and inhibitory function in the hippocampus. *Endocrinology*. 148:92–102.

Groeneweg S, Peeters RP, Moran C, Stoupa A, Auriol F, Tonduti D, Dica A, Paone L, Rozenkova K, Malikova J *et al*. 2019. Effectiveness and safety of the tri-iodothyronine analogue Triac in children and adults with MCT8 deficiency: an international, single-arm, open-label, phase 2 trial. *Lancet Diabetes Endocrinol*. 7:695–706.

Groeneweg S, van Geest FS, Peeters RP, Heuer H, Visser WE. 2020. Thyroid hormone transporters. *Endocr Rev*. 41:bbz008.

Heuer H, Schafer MK, O'Donnell D, Walker P, Bauer K. 2000. Expression of thyrotropin-releasing hormone receptor 2 (TRH-R2) in the central nervous system of rats. *J. Comp. Neurol*. 428:319–336.

Johansson PA. 2014. The choroid plexuses and their impact on developmental neurogenesis. *Front Neurosci*. 8:340.

Kelsom C, Lu WG. 2013. Development and specification of GABAergic cortical interneurons. *Cell and Bioscience*. 3:19.

Kessaris N, Fogarty M, Iannarelli P, Grist M, Wegner M, Richardson WD. 2006. Competing waves of oligodendrocytes in the forebrain and postnatal elimination of an embryonic lineage. *Nat Neurosci*. 9:173–179.

Levitt P, Eagleson KL, Powell EM. 2004. Regulation of neocortical interneuron development and the implications for neurodevelopmental disorders. *Trends Neurosci*. 27:400–406.

Lopez-Espindola D, Morales-Bastos C, Grijota-Martinez C, Liao XH, Lev D, Sugo E, Verge CF, Refetoff S, Bernal J, Guadano-Ferraz A. 2014. Mutations of the thyroid hormone transporter MCT8 cause prenatal brain damage and persistent hypomyelination. *J Clin Endocrinol Metab*. 99:E2799–E2804.

Madisen L, Zwingman TA, Sunkin SM, Oh SW, Zariwala HA, Gu H, Ng LL, Palmiter RD, Hawrylycz MJ, Jones AR *et al*. 2010. A robust and high-throughput Cre reporting and characterization system for the whole mouse brain. *Nat Neurosci*. 13:133–140.

Mayerl S, Muller J, Bauer R, Richert S, Kassmann CM, Darras VM, Buder K, Boelen A, Visser TJ, Heuer H. 2014. Transporters MCT8 and OATP1C1 maintain murine brain thyroid hormone homeostasis. *J Clin Invest*. 124:1987–1999.

Mayerl S, Schmidt M, Doycheva D, Darras VM, Huttner SS, Boelen A, Visser TJ, Kaether C, Heuer H, von Maltzahn J. 2018. Thyroid Hormone Transporters MCT8 and OATP1C1 Control Skeletal Muscle Regeneration. *Stem Cell Reports*. 10:1959–1974.

Mayerl S, Visser TJ, Darras VM, Horn S, Heuer H. 2012. Impact of Oatp1c1 deficiency on thyroid hormone metabolism and action in the mouse brain. *Endocrinology*. 153:1528–1537.

Nery S, Wichterle H, Fishell G. 2001. Sonic hedgehog contributes to oligodendrocyte specification in the mammalian forebrain. *Development*. 128:527–540.

Powell EM. 2013. Interneuron development and epilepsy: early genetic defects cause long-term consequences in seizures and susceptibility. *Epilepsy Curr*. 13:172–176.

Rallu M, Machold R, Gaiano N, Corbin JG, McMahon AP, Fishell G. 2002. Dorsoventral patterning is established in the telencephalon of mutants lacking both Gli3 and Hedgehog signaling. *Development*. 129:4963–4974.

Remerand G, Boespflug-Tanguy O, Tonduti D, Touraine R, Rodriguez D, Curie A, Perreton N, Des Portes V, Sarret C, Rmlx Ahds Study Group. 2019. Expanding the phenotypic spectrum of Allan-Herndon-Dudley syndrome in patients with SLC16A2 mutations. *Dev Med Child Neurol*. 61:1439–1447.

Reyns GE, Janssens KA, Buyse J, Kuhn ER, Darras VM. 2002. Changes in thyroid hormone levels in chicken liver during fasting and refeeding. *Comp Biochem Physiol B Biochem Mol Biol*. 132:239–245.

Richard S, Guyot R, Rey-Millet M, Prieux M, Markossian S, Aubert D, Flamant F. 2020. 'A pivotal genetic program controlled by thyroid hormone during the maturation of GABAergic neurons. i*Science*. 23:100899.

Rossignol E. 2011. Genetics and function of neocortical GABAergic interneurons in neurodevelopmental disorders. *Neural Plast*. 2011:649325.

Schwartz CE, May MM, Carpenter NJ, Rogers RC, Martin J, Bialer MG, Ward J, Sanabria J, Marsa S, Lewis JA et al. 2005. Allan-Herndon-Dudley syndrome and the monocarboxylate transporter 8 (MCT8) gene. *Am J Hum Genet*. 77:41–53.

Trajkovic-Arsic M, Muller J, Darras VM, Groba C, Lee S, Weih D, Bauer K, Visser TJ, Heuer H. 2010. Impact of monocarboxylate transporter-8 deficiency on the hypothalamus-pituitary-thyroid axis in mice. *Endocrinology*. 151:5053–5062.

Trajkovic M, Visser TJ, Mittag J, Horn S, Lukas J, Darras VM, Raivich G, Bauer K, Heuer H. 2007. Abnormal thyroid hormone metabolism in mice lacking the monocarboxylate transporter 8. *J Clin Invest*. 117:627–635.

Uchida K, Taguchi Y, Sato C, Miyazaki H, Kobayashi K, Kobayashi T, Itoi K. 2014. Amelioration of improper differentiation of somatostatin-positive interneurons by triiodothyronine in a growth-retarded hypothyroid mouse strain. *Neurosci Lett*. 559:111–116.

Vancamp P, Deprez MA, Remmerie M, Darras VM. 2017. Deficiency of the thyroid hormone transporter monocarboxylate transporter 8 in neural progenitors impairs cellular processes crucial for early corticogenesis. *J Neurosci*. 37:11616–11631.

Wallis K, Sjogren M, van Hogerlinden M, Silberberg G, Fisahn A, Nordstrom K, Larsson L, Westerblad H, Morreale de Escobar G, Shupliakov O *et al*. 2008. Locomotor deficiencies and aberrant development of subtype-specific GABAergic interneurons caused by an unliganded thyroid hormone receptor alpha1. *J Neurosci*. 28:1904–1915.

Wiersinga WM, Chopra IJ. 1982. Radioimmunoassay of thyroxine (T4), 3,5,3′-triiodothyronine (T3), 3,3′,5′-triiodothyronine (reverse T3, rT3), and 3,3′-diiodothyronine (T2). *Methods Enzymol*. 84:272–303.

Wonders CP, Anderson SA. 2006. The origin and specification of cortical interneurons. *Nat Rev Neurosci*. 7:687–696.

Xu Q, Cobos I, De La Cruz E, Rubenstein JL, Anderson SA. 2004. Origins of cortical interneuron subtypes. *J Neurosci*. 24:2612–2622.

Xu Q, Guo L, Moore H, Waclaw RR, Campbell K, Anderson SA. 2010. Sonic hedgehog signaling confers ventral telencephalic progenitors with distinct cortical interneuron fates. *Neuron*. 65:328–340.

Xu Q, Tam M, Anderson SA. 2008. Fate mapping Nkx2.1-lineage cells in the mouse telencephalon. *J Comp Neurol*. 506: 16–29.

Xu Q, Wonders CP, Anderson SA. 2005. Sonic hedgehog maintains the identity of cortical interneuron progenitors in the ventral telencephalon. *Development*. 132:4987–4998.